

Analytical Study on the Visibility of Potential Positions for External Human-Machine Interfaces

Jose Gonzalez-Belmonte^{1,2} and Jaerock Kwon^{1*}

^{1*}Electrical and Computer Engineering, University of Michigan-Dearborn, 4901 Evergreen Rd, Dearborn, 48128, Michigan, United States of America.

²Math and Computer Science, Lawrence Technological University, 21000 W Ten Mile Rd, Southfield, 48076, Michigan, United States of America.

*Corresponding author(s). E-mail(s): jrkwon@umich.edu;
Contributing authors: josegonz@umich.com;

Abstract

As we move towards a future of autonomous vehicles, questions regarding their method of communication have arisen. One of the common questions concerns the placement of the signaling used to communicate with pedestrians and road users, but little work has been published fully dedicated to exploring this. This paper uses a simulation made in the Unity game engine to record the visibility of fifteen different vehicles under fifty-seven different scenarios each for the first time, specifically regarding the visibility of frontal elements by a pedestrian on the sidewalk. Variables include the vehicle type, position, number of vehicles on the road, and minimum and maximum distance of the recorded points. It was concluded that the areas of the vehicle most often seen by pedestrians on the sidewalk attempting to cross the road were the wheels, front fenders, front bumper, and side mirrors. Suggestions are made to implement multiple eHMI to address pedestrian behavior. These findings are valuable in the future design of signaling for autonomous vehicles in order to ensure pedestrians are able to see them on approaching vehicles. The software used provides a platform for similar works in the future to be conducted.

Keywords: autonomous vehicles, eHMI, road safety, pedestrian safety

1 Introduction

In the field of Autonomous Vehicles (AVs), external human-machine interfaces (eHMIs) refer to methods of communication, such as screens or lights, that an AV can use to communicate with other road users. With traditional vehicles, drivers are able to use body language to communicate implicitly with pedestrians, but the introduction of AVs introduces a “social void” through the removal of an attentive human driver who can handle ambiguous road interactions ([1]). eHMIs were introduced as a solution to this problem, aiming to eliminate ambiguity and the necessity of inter-personal social cues by letting the AV outwardly express its intent to pedestrians explicitly.

Previous studies have addressed the effectiveness of eHMIs ([2–4]) and the symbols they should use ([1]), but few studies have been focused on determining the ideal position for these displays. Those available are concerned primarily with the behavior and perception of the pedestrian ([1, 5, 6]), but few have attempted to optimize the position of the display to maximize its visibility, and the ones to do so are limited in the data collected and represented ([7]). As a result, there exists a gap in the knowledge of eHMI placement, including information on where it will be most seen by pedestrians, how distance may affect its visibility, and how the type of vehicle may limit these choices. As observers must be able to perceive an eHMI before making a decision based on its information, this gap is must be filled in order to set standards for the technology.

The present study aims to contribute answer these questions with a data-capturing method that measures the visibility of different vehicle parts and applies it to a wide variety of scenarios and vehicles. The intent is to develop an open-source software capable of simulating the possible positions for a vehicle and produce a heatmap indicating what parts and areas of the vehicle were visible in the highest amount of scenarios, then utilize this tool with a variety of vehicle types and layout permutations in order to determine general recommendations for eHMI placement based on the results.

2 Related Work

The effectiveness of eHMIs has been thoroughly investigated through experiments using virtual reality ([2]), video-based eye tracking techniques ([5, 6]), the Wizard of Oz method ([3]), and outdoor experiments with real autonomous vehicles ([4]). In each of these examples the presence of an eHMI proved to increase response time and feelings of safety on pedestrians. However each these experiments feature vastly different proposals of eHMIs, often varying in their positioning within the same study. Research on the positioning of eHMI is less common than those focused on their effectiveness.

Dey et al. [6] had participants stand on a sidewalk wearing eye tracking glasses, and indicate their willingness to cross as four vehicles approached the pedestrian crossing in front of them. The experiment found that pedestrians lose their willingness to cross the road when the vehicle is at a distance of 40 m from them, and that the part of the vehicle they focus on varies as a function of the vehicle’s distance, moving from the vehicle bumper to the windshield as it approaches. This suggests that a distributed

approach to eHMI design is required, as pedestrian attention shifts thorough their interaction with an autonomous vehicle.

de Winter et al. [8] conducted an experiment where participants walk around a busy parking lot with an eye tracking device, and found that most participants focus on the general parts of a vehicle that are affected by their movement, such as the vehicle’s front, back, and wheels. A significant portion of pedestrians also looked at the windshield of the vehicle, in accordance with [6]. This study also concluded that eHMIs must be visible from all angles due to the varied conditions in which pedestrians encounter them.

Guo et al. [5] used an eye tracking device as well. In this experiment participants watched a video of a vehicle approaching from the right, while their gaze was being recorded, in order to determine what parts of the vehicle they paid attention to. The vehicles illustrated in this experiment either employed no eHMI, or showed one of six different eHMI designs (flashing text, sweeping pedestrian icon, sweeping arrow, flashing smiley, flashing light band, and sweeping light bar) located in one of three different positions (grill, windshield, and roof). The results determined the windshield to be the locations of the vehicle with the longest visual attention from participants, followed closely by the grill, but found little difference in the efficiency of an eHMI based on said location.

A similar experiment to the one done for the present paper is that of Troel-Madec et al. [7], where a 3D simulation was created to measure what parts of the vehicle were visible most of the time to pedestrians looking at an incoming vehicle, and hence which areas were best suited for the placement of eHMIs. For this, the team placed three 3D models of a sedan vehicle in a virtual space, forming an unmoving line on the side closest to the sidewalk and facing towards the camera. Each vehicle was then assigned a different primary color, with differences in the shading based on what part of the vehicle they were in: front, side, and back. A virtual camera then took a series photos from a predefined set of points on the sidewalk at five different heights, in order to simulate how children, teenagers, and adults may perceive the situation. The pixels on the resulting images were analyzed, using the solid color of the vehicles to find what parts of the each vehicle were visible the most. The results pointed to the side of the vehicle to be the most consistently visible part of the vehicle, and the team used these results to develop a prototype for an eHMI that was positioned on the front doors and windshield rails.

These studies overall conclude that the specific location of an eHMI matters less than the fact said eHMI is visible to the observer ([2]), and that pedestrians tend to fixate on parts of the vehicle such as the bumper, the windshield, the wheels, and the general back and front, while the sides of the vehicle seem to be the general area most visible in most scenarios. While these results are promising, they lack granularity and are always done with a single type of vehicle, often coming from the same direction.

This paper aims to find the place on an incoming vehicle most visible to most pedestrians in most situations, similar to the results presented in [7], while widening the scope to include a variety of vehicle types and scenarios not tested in the previous literature.

3 Methods

The following requirements must be met by the results in order to provide a specific visible area for the placement of eHMIs:

1. The raw data must be granular, not just pointing at general parts of the car, but showing how visible specific points on the surface of the vehicle are.
2. Since pedestrians may find their view of a vehicle blocked by a nother (e.g. when vehicles are in a line), the software must be able to calculate all possible scenarios where this may happen and simulate them.
3. Multiple vehicles of different sizes must be simulated, as different vehicle types may present different challenges and limitations for eHMI design.
4. Vehicles may come from four possible directions, respective to the sidewalk: two perpendicular to it, and two parallel to it. The simulation must present cases where this can be explored.

A simulation software was created to achieve these goals using the Unity game engine. The execution of a simulation can be divided into a hierarchy of five levels, each made up of the ones after:

1. A *Simulation Run* is the highest level, where the user provides the program with the parameters that it will use during the simulation. These include:
 - The set of positions on the virtual road where camera may be positioned (*Camera Positions*) and the directions that the camera may face at each (*Camera Directions*).
 - The set of positions on the virtual road that the *Target Vehicle* may occupy. This is the vehicle that is being measured, and the only one to record whenever it is visible to the camera.
 - The type of vehicle used for the *Target Vehicle*, each corresponding to a pre-selected 3D model implemented into the program.
 - The set of positions that the *Filler Vehicles* may occupy. These are other vehicles placed on the scene that do not record data, and only exist to block the view of the *Target Vehicle* from the camera as illustrated in Fig.1.

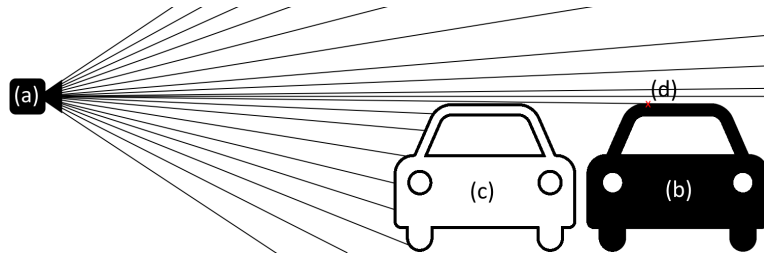


Fig. 1 Diagram showing the camera (a) attempting to capture points on the surface of the *Target Vehicle* (b) but being blocked by a *Filler Vehicle* (c). Only a single point (d, marked with an X) can be seen being recorded.

- The type of vehicle used for the *Filler Vehicles*.

- The number of vehicles in the scenario, including the *Target Vehicle* and *Filler Vehicles*. There will always be one and only one *Target Vehicle* in any given simulation. There may never be more *Filler Vehicles* in the road than there are positions for it. Entering '1' will make it so no *Filler Vehicles* are ever present in the simulation.
- The minimum and maximum distance that a point on the *Target Vehicle* must be from the camera to be recorded.

Based on these parameters, the software will instantiate a *Target Vehicle* in the pre-made environment, calculate all possible permutations of the *Target Vehicle* and the *Filler Vehicles* in their possible positions, then cycle through each of these *Scenarios* using the specified settings.

2. A *Scenario* represents a combination of different placements on the road for the *Target Vehicle* and other *Filler Vehicles* on the road. Since we want to find the points of the *Target Vehicle* that are visible the most often, we want to cycle through all possible combinations of *Filler Vehicle* placements to simulate the ways in which other vehicles on the road may block the view of the pedestrian.
3. For each *Scenario*, the camera will cycle through each of the *Camera Positions*. For this paper, these all correspond to positions where a pedestrian may be located on the left sidewalk, although the program has capability to select positions on the road as well.
4. For each *Camera Direction* available at each *Camera Position*, the camera executes a series of *Data Captures* at five different heights from the floor: 1m, 1.2m, 1.4m, 1.6m, and 1.8m.
5. To perform a *Data Capture*, the camera simulates a series of ray-casts in a grid pattern coming from the camera to replicate where it is observing the *Target Vehicle*. Each ray-cast starts at the minimum distance away from the camera, and ends at its maximum distance. Ray-casting allows us to find the intersection point between an origin point and a destination point, as well as the details of the first collider hit this way, such as what object it belongs to or what components are attached to that game object ([9]). An example of this process can be seen in Fig. 2.

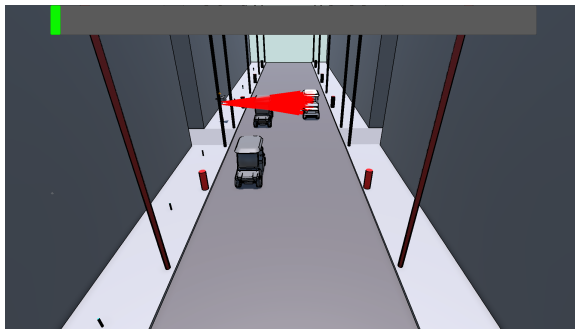


Fig. 2 Screenshot of the simulation running. Red lines indicate the trajectory of the ray-casts that have hit the *Target Vehicle*.

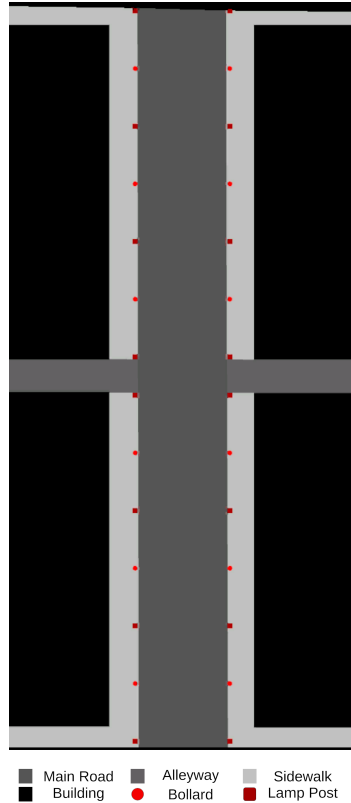


Fig. 3 Top-Down View of the Virtual Street Layout.

The virtual environment for this simulation, as seen on Fig. 3, consists of a two-way street with alleyways intersecting it from the left and the right. The main road in this virtual intersection is 6.94m wide and 57.719m long; the alleyways are 2.604m wide; both sidewalks are 2.216m wide and 0.102m above the road; the four cuboids that stand for buildings in this model are each 21.5m tall, and cover the space not occupied by the alleyways or the road.

The virtual sidewalk was also populated by static objects that serve as obstacles in the observer's view. There are two kinds of obstacles, each placed in alternate order on the sidewalk 4.5m from each other. Both sidewalks are mirrored.

- **Bollards:** Each a cylinder 0.305m in radius and 0.914m in height. No cylinder is placed in the space taken by an alleyway intersecting a sidewalk. All cylinders are positioned 0.063m away from the edge of the curb. There are a total of 12 bollards on the scene. Visible as red circles in Fig. 3.
- **Lamp Posts:** A series of tall cylinders representing lamp posts placed on the sidewalk, 0.161m from the edge. Each tall cylinder is 0.152m in radius and 9m in height. Six are placed on each sidewalk, 9m from each other. There are a total of 16 lamp posts on the scene. Visible as red squares in Fig. 3.

The vehicles to be used in this simulation had to be representative of the variety of vehicles that can be found on the road. The fifteen vehicles seen in Table 1 were selected, using the list of vehicle types outlined by the [10] as a base. All models were found and downloaded for free from the online website Sketchfab.com under the Creative Commons license. Each model, the vehicle type it corresponds to, and its closest real-life equivalent can be seen in Table 1, with notes providing additional context if the specific model was not specified.

Table 1 List of vehicles used in the simulations.

Category	Model	Source	Notes
Motorcycle	Honda Shadow RS 2010	[11]	
Smart Car	Smart Fortwo	[12]	
Carryall Car	N/A	[13]	Described as a "Golf Cart"
Sedan	N/A	[14]	Described as "Based on asian design features of last decade [2010s]."
SUV	Ford Edge 2006	[15]	
Panel Van	D3S MB Vito Panel Van (W447) '15	[16]	
Topless Convertible	N/A	[17]	Chrysler Sebring Convertible. Specific model not specified. Page removed.
Station Wagon	80s Lincoln Zephyr Mercury	[18]	
Four wheel Truck	N/A	[19]	Described as a generic Japanese-made small-cabin commercial truck from the 90s.
Minibus	Peugeot J5	[20]	
Pickup Truck	2015 Ford F150 King Ranch Edition	[21]	
Moving Truck	N/A	[22]	Described as a generic Japanese-made 2-door pickup-cabin box truck.
Motor home	N/A	[23]	Described as a "Modified GMC Motorhome"
Double Decker Bus	N/A	[24]	Described as a "Hong Kong Bus", corresponding to a Volvo B8L
Single Decker Bus	N/A	[25]	

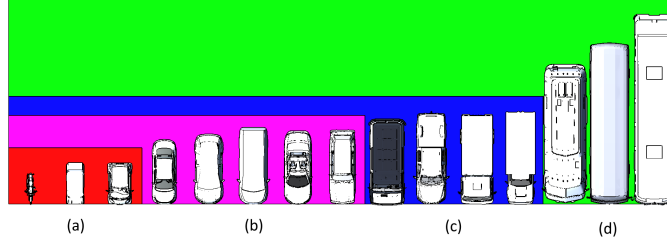


Fig. 4 Top-Down View of the fifteen vehicles used in the simulations. Color denotes the category of each vehicle: (a) Small (b) Medium (c) Large (d) Extra Large

Based on their dimensions, the vehicles selected were broken into four categories, based on their length and classification in [10]:

- **Small (S):** Vehicles of Class 1 and vehicles of Class 2 less than 4m in length (Fig. 4(a)).
- **Medium (M):** Vehicles of Class 2 and Class 3 between 4m and 6m in length (Fig. 4(b)).
- **Large (L):** Vehicles of Class 3, Class 4, and Class 5 between 6m and 8m in length (Fig. 4(c)).
- **Extra Large (XL):** Vehicles of Class 4, Class 5, and Class 6 longer than 8m (Fig. 4(d)).

Since all vehicle models were made by a third-party, it is important to compare the dimensions of the virtual vehicles with the real counterpart of those vehicles to ensure accuracy. Adjustments were made to the size of the vehicles to more closely resemble their real-life equivalents. A comparison of both can be see in Table 2.

Table 2 Dimensions of the virtual vehicles and their real-life equivalents, in meters.

Vehicle Size Category	Real Life Dimensions (m)			Dimensions in Simulation (m)		
	H	W	L	H	W	L
Motorcycle	1.13	0.92	2.51	1.15	0.86	2.14
Smart Car	1.54	1.56	2.70	1.71	1.88	2.78
Carryall Car	-	-	-	1.78	1.22	2.79
Sedan	-	-	-	1.44	1.71	4.35
SUV	1.70	1.93	4.72	1.63	2.08	4.71
Panel Van	1.90	1.93	4.90	1.91	1.91	4.89
Topless Convertible	-	-	-	1.31	1.93	4.94
Station Wagon	1.38	1.80	4.97	1.36	1.83	4.98
Four wheel Truck	2.92	1.97	4.77	2.61	2.84	6.02
Minibus	2.42	1.97	5.49	2.46	2.62	5.81
Pickup Truck	2.00	2.03	6.18	1.86	2.35	6.03
Moving Truck	-	-	-	2.46	2.09	6.25
Motor home	-	-	-	3.21	3.02	9.12
Double Decker Bus	-	-	-	4.79	2.77	11.10
Single Decker Bus	-	-	-	3.12	3.17	12.80

The program has eight possible positions for vehicles.

- **On the Road:** Three of the positions are on the left side (Fig. 5(a to d)(1 to 3)) and three on the right side (Fig. 5(a to d)(5 to 7)). Vehicles in each set of positions face in the same direction, forming a line. For this work, the American driving direction was used (right side), so vehicles on the left side of the image drive towards the south, while those on the right side drive northward.
- **Exiting Alleyway:** Two of the positions place the vehicle intersecting with the sidewalk, facing east (Fig. 5(a to d)(4)) or west (Fig. 5(a to d)(8)) towards the road. This emulates vehicles turning into the road, as well as vehicles driving across the intersection.

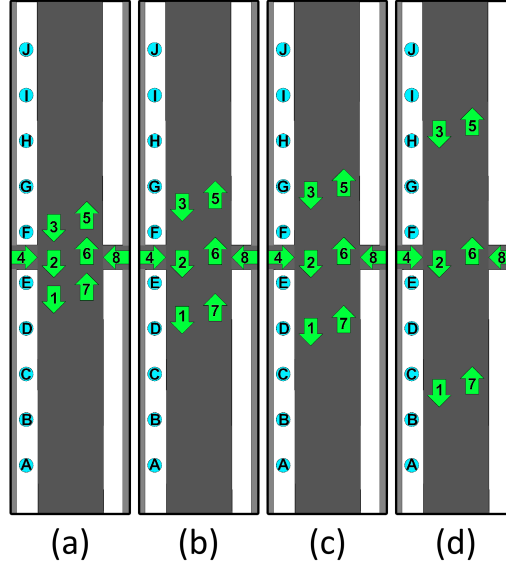


Fig. 5 Diagram illustrating the ten possible sidewalk camera positions, and the eight possible vehicle positions, based on the size categories of the target vehicle. (a) Small vehicles (b) Medium vehicles (c) Large vehicles (d) Extra large vehicles.

The front of the spawned vehicles are aligned with the pivot point they are placed in. To ensure that vehicles wouldn't overlap, the specific position of each of the six pivots on the main road varies depending on the size of the vehicle being evaluated. Table 3 shows the distance between pivots for each size category, while Fig. 5 illustrates them.

This means that the space between the front of a vehicle, and the back of the one its facing will vary between vehicles. Table 4 shows what this distance is for all fifteen vehicles used in the simulation.

At any given time, one and only one of the vehicles currently in the environment may record the points where it is being observed by the recording camera, this is considered the *Target Vehicle*. In each *Scenario*, the rest of the spaces that are occupied

Table 3 Distance between each vehicle position on the road

Vehicle Category	Distance (m)
Small	3.792
Medium	5.970
Large	7.240
Extra Large	13.730

Table 4 Distance between each vehicle when forming a line on the same lane.

Category	Vehicle Type	Bumped-to-Bumper Distance (m)	Vehicle Length (m)
Small	Motorcycle	1.65	2.14
Small	Smart Car	1.01	2.78
Small	Carryall Car	1.00	2.79
Medium	Sedan	1.62	4.35
Medium	SUV	1.26	4.71
Medium	Panel Van	1.08	4.89
Medium	Topless Convertible	1.03	4.94
Medium	Station Wagon	0.99	4.98
Large	Four wheel Truck	1.22	6.02
Large	Minibus	1.43	5.81
Large	Pickup Truck	1.21	6.03
Large	Moving Truck	0.99	6.25
Extra Large	Motor home	4.61	9.12
Extra Large	Double Decker Bus	2.63	11.10
Extra Large	Single Decker Bus	0.93	12.80

by vehicles are all filled with *Filler Vehicles* that use the same model as the *Target Vehicle*, but do not record any data.

Because the position of a vehicle on the road will vary regularly, and hence parts of said vehicle may be blocked by another vehicle, the simulation generates all possible combinations of *Target Vehicle* and *Filler Vehicle* positions, based on whether a position is occupied by the target vehicle, a filler vehicle, or no vehicle.

The simulation has a single camera that, through a series of *Data Captures*, records what parts of the *Target Vehicle* are being observed. During the simulation, the camera cycles through a list of *Camera Positions*, their possible *Camera Directions*, and their possible heights. All *Camera Positions* are placed on the sidewalk, 1.2m from the street, and are almost all spaced out from the next by 4.84m, except for the two adjacent to the alleyway which are 5.38m apart from each other. The *Camera Positions* can be seen in Fig. 5 (A to J).

When the camera is at a specific *Camera Position*, it must take a *Data Capture* for each possible facing that a road user may have in that position. To replicate this, each point has a list of valid facing directions that the camera cycles through, and that the user selects during setup. Since the environment used for this simulation is made

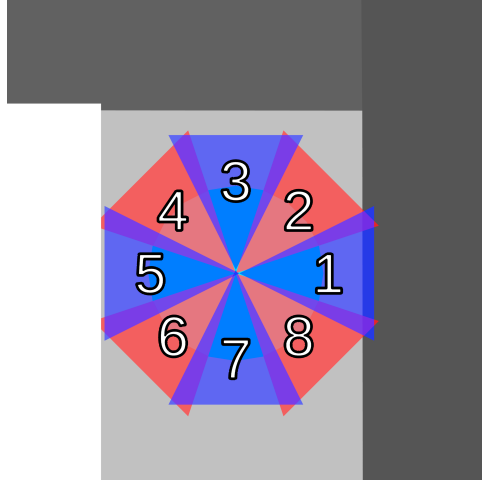


Fig. 6 Diagram illustrating the eight *Camera Directions* that a camera may take at any given *Camera Position*, each identified by a the cardinal or ordinal direction relative to the overhead camera: East (1), North-East (2), North (3), North-West (4), West (5), South-West (6), South (7), and South-East (8).

up entirely of right angles, the *Camera Directions* are implemented in increments of 45degrees, as seen in Fig. 6

Since our roads are shared with people of varied heights, the camera needs to get *Data Captures* from different heights. For each *Camera Direction*, the camera cycles through five camera heights: 1.0m, 1.2m, 1.4m, 1.6m, and 1.8m. These correspond to the ones used by [7] to simulate a variety of age groups. According to the United States of America’s National Center for Health Statistics [26], these would approximately match the height of the median American at the ages of 3, 6, 10, 13, and 20 years old respectively.

The system for recording data during a *Data Capture* is mainly controlled by three scripts: The *Heatmap Sender*, placed on the camera; the *Heatmap Display* placed on the *Target Vehicle*; and the the *Heatmap Receiver*, placed also on the *Target Vehicle*.

In each *Data Capture*, the *Heatmap Sender* casts a total of 14 400 straight rays in a 160×90 grid pattern. This resolution was chosen for two reasons:

1. Ray-casting is very resource intensive, so a lower resolution was needed to ensure the simulation times remained achievable and in-scope.
2. During development 1920×1080 was the most common screen resolution, according to W3Counter [27]. Since the Camera component in Unity makes use of the application resolution, and 1920 and 1080 can be divided evenly by 160 and 90 respectively, this reduces effect of rounding on the results.

At the start of the simulation, the *Heatmap Display* simplifies the mesh of the *Target Vehicle* into a tridimensional array of *Grid Points*, where each is a structure containing the internal local coordinates of that point on the grid. Each *Grid Point* also holds a long integer value representing how many times that point has been hit by the *Heatmap Sender*. All points in the grid are in contact with the mesh of the vehicle.

This system is used to round the information received for later display. Note that, by using collisions and ray-casting as the methods of capturing data, the simulation is only capable of capturing the visibility of points in the geometry of the vehicle, and does not account for factors such as reflectiveness and color.

When one of the rays casted by the *Heatmap Sender* hits the the *Target Vehicle*, the tridimensional point of contact is recorded internally in local coordinates by the *Heatmap Receiver*. These rays are cast in the facing direction of the camera using Unity’s *ScreenPointToRay* function, which adjusts for the camera’s default 60 degree field of view. At the end of each *Data Capture*, once all rays have been cast by the *Heatmap Sender*, the *Heatmap Display* rounds each of the points recorded to the nearest equivalent *Grid Point* (if applicable). Every time a point on the *Heatmap Receiver* is rounded to a *Grid Point*, the value associated with said *Grid Point* is increased by one.

Since the projection of the ray-casts is meant to simulate viewing, it is affected by the Inverse Square Law just like light is, making it so points are proportionately farther apart from other points in the same radius based on the squared distance from the camera [28]. This introduces a proximity bias, making it so whenever the camera is closer to the *Target Vehicle*, multiple local coordinates found by the *Heatmap Sender* during a *Data Capture* would be rounded to the same *Grid Point*. To prevent this, it was made so *Grid Points* may only increase their value by one during a given *Data Capture*.

Once the simulation has run through all *Scenarios*, the points stored and their associated values are serialized into a JavaScript Object Notation (JSON) file that can be read by the software. This represents the end of the simulation. In a separate Unity scene, the software is able to load said JSON files, then the user may select one or more of the JSON files to display, as well as one of the fifteen vehicles to display it on (Table 1). The software will then instantiate a copy of the selected vehicle and add the data from the JSON files to that vehicle’s Heatmap Display through an additive process. The value of each *Grid Points* is then normalized with the highest value in the file, and evaluated to give each point one of eight colors corresponding to their normalized value, as seen on Fig. 7.

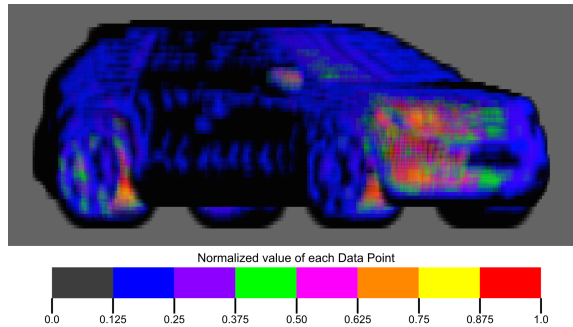


Fig. 7 Diagram illustrating the coloring of *Grid Points* based on their normalized value, with the highest value recorded as the upper limit.

The resulting 3D visualization is then presented to the user so they can inspect it and take virtual photographs of the vehicle facing nine of its possible angles: front, front-right corner, right flank, back-right corner, back, front-left corner, left flank, front-left corner, and directly from above.

4 Experiment Setup

The software developed for the simulation was made using the Unity game engine, version 2022.3.28f1, and C#. Blender 4.2 was used to model the street, as well as adjust the pivot and size of the vehicles. Most of the data capture process was done using Unity's built-in physics and collision system for its ray-casting functionality. Physics were not used for anything else.

Since the amount of filler vehicles on the road will influence how much of the *Target Vehicle* is visible, multiple *Simulation Runs* were done varying the number of *Filler Vehicles* on the road. Fig. 8 illustrates the configuration of all positions that *Target Vehicles* and *Filler Vehicles* occupied for this experiment, depending on their type.

- The total amount of vehicles may be between 1 and 4 for scenarios where the *Target Vehicle* is on the road closest to the sidewalk (Fig. 8 (a, e, j, n)(1,2,3)). This is because visibility in that case may only be affected by *Filler Vehicles* placed on the sidewalk (Fig. 8 (a, e, j, n)(4)) or in front of the *Target Vehicle*.
- The total amount of vehicles is always 1 when the *Target Vehicle* is located on the west alleyway (Fig. 8 (b, f, j, n)(4)), since there is no position where *Filler Vehicles* may block it.
- The total amount of vehicles may be between 1 and 7 when the *Target Vehicle* is located on the right-hand side of the road (Fig. 8(c, g, k, o)(5,6,7)), since it may be blocked by other vehicles in those positions, as well as vehicles on the left side (Fig. 8 (c, g, k, o)(1 to 4)).
- The total amount of vehicles may be between 1 and 8 when the *Target Vehicle* is positioned on the east alleyway (Fig. 8 (d, h, l, p)(8)), since it can be blocked by any other vehicle on the road.

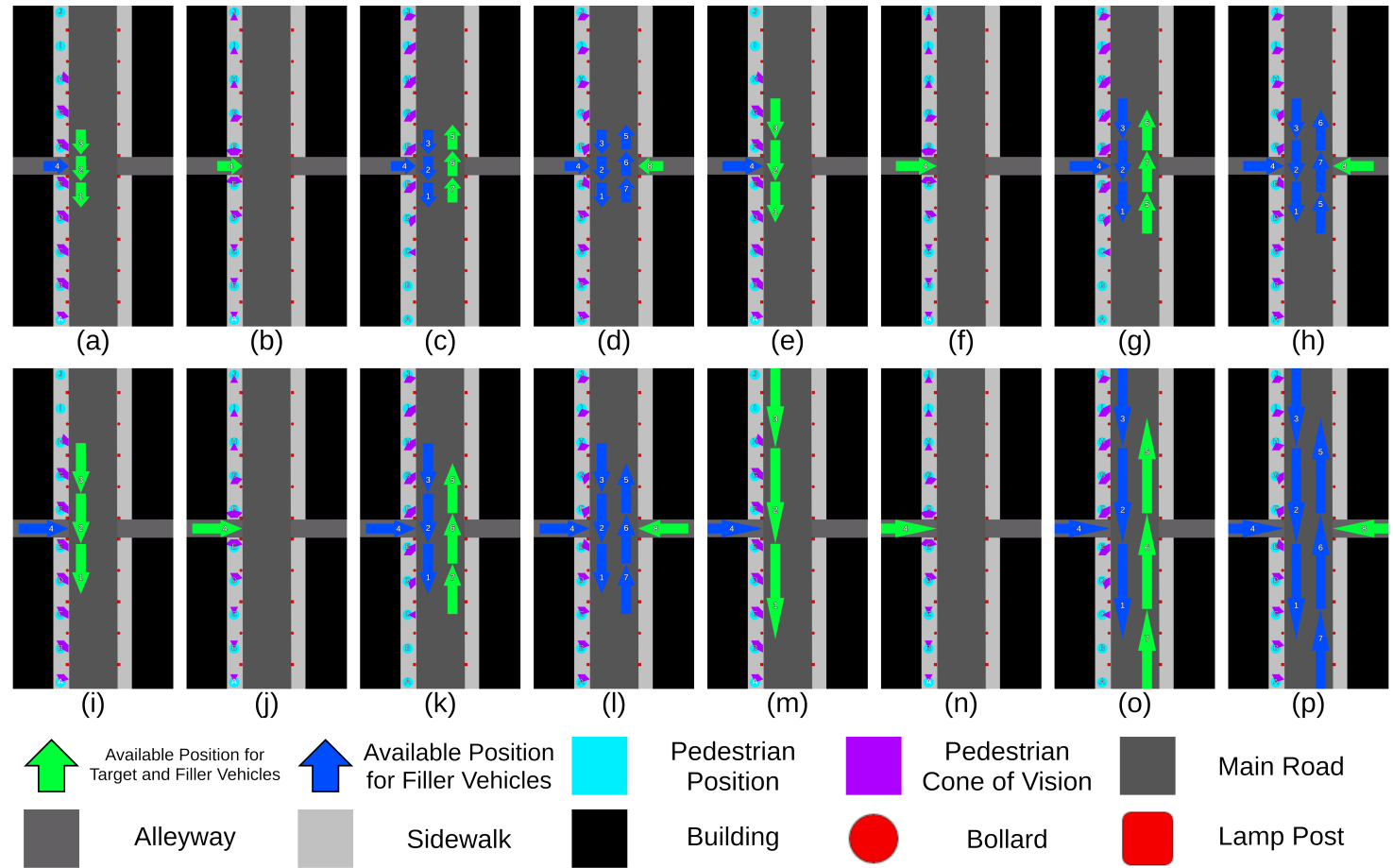


Fig. 8 Diagram illustrating all sixteen setups based on the *Target and Filler Vehicle* available positions (green arrows in (a) to (p)), exclusive *Filler Vehicle* available positions (blue arrows in (a) to (o)), vehicle type ((a) to (d) for Small, (e) to (h) for Medium, (i) to (l) for Large, (m) to (p) for Extra Large), *Camera Positions* ((a to p)(A to J)), and *Camera Directions* (Marked in purple).

Each *Camera Position* has a total of ten possible positions on the sidewalk that it may cycle through (Fig. 8(a to p)(A to J)). The user may chose which ones to use for a *Simulation Run*, as well as the direction the camera may face at said location. For the simulations in this paper, camera positions were chosen based on four possible vehicle facings, minimizing cases where the pedestrian would not be able to see the front of the vehicle:

- If the *Target Vehicle* is going southwards, *Data Captures* will only happen towards the east, north-east, and north directions (Fig. 8 (a, e, i, m), Fig. 6(1,2,3)).
- If the *Target Vehicle* is coming out of the left alleyway, going eastwards, *Data Captures* will only be made in the north, north-east, south, and south-east directions (Fig. 8 (b, f, j, n), Fig. 6(2,3,7,8)).
- If the *Target Vehicle* is going northwards, *Data Captures* will only be made in the east, south-east, and south directions (Fig. 8 (c, g, k, o), Fig. 6(1,7,8)).
- If the *Target Vehicle* is coming out of the right alleyway, going westwards, *Data Captures* will only happen towards the north, north-east, south, and south-east (Fig. 8 (d, g, l, p), Fig. 6(2,3,7,8)).

For this experiment, in order to produce data on how the distance between the *Target Vehicle* and the camera may affect the visibility of certain elements, each set of nineteen scenarios was run three times with different minimum and maximum distances for the *Data Capture*: 0m to 5m, 5m to 25m, and 25m to 75m. Fig. 9 puts these values into scale within the environment of the simulation.

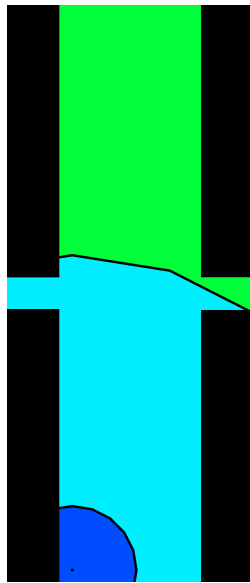


Fig. 9 Visualization of the three ranges used for *Data Capturing* for this experiment: Blue: 0m to 5m; Cyan: 5m to 25m; Green: 25m to 75m.

The simulation was run a total of nineteen times for each vehicle, producing 855 output files. *Simulation Runs* were done in two computers at the same time, each running multiple parallel instances of the program. The main computer used for these simulations was a desktop personal computer equipped with an AMD Ryzen 7 2700 eight-core processor, an NVIDIA GeForce RTX 2060, and 16 GB of RAM running a 64-bit version of Windows 10. The second computer was an Acer Nitro V 15 laptop equipped with a 13th gen Intel Core i7-13620H, an NVIDIA GeForce RTX 4060 Laptop GPU, and 16 GB of RAM running a 64-bit version of Windows 11 Home.

The time taken by each *Simulation Run* varied from 1 minute to 8 hours, depending on factors such as:

- The size of the model, as larger models were hit by more ray-casts.
- The amount of polygons in the model, which takes up more resources to render.
- The number of vehicles and possible vehicle positions, as a low number of the former with a higher number of the later means more permutations to test.
- The total number of *Camera Directions* visited by the *Data Captures*.

5 Results and Discussion

A total of 855 separate simulations were run in order to produce data that could represent the visibility of all fifteen selected vehicles under the three different ranges. Since the number of *Scenarios* varies depending on the position of the vehicle, simply adding all files corresponding to a given vehicle type would produce results biased towards scenarios where the vehicle was on the right side of the street, since those have a higher amount of *Filler Vehicle* positions and permutations. Because of this, results were divided into four categories to be processed and normalized independently:

- Vehicle is facing south (Fig. 8 (a,e,i,m)).
- Vehicle is facing east (Fig. 8 (b,f,j,n)).
- Vehicle is facing north (Fig. 8 (c,g,k,o)).
- Vehicle is facing west (Fig. 8 (d,h,l,p)).

For each category, the recorded data was divided into subsets based on their minimum and maximum distance parameters, then each subset was added into a heatmap showing the visibility of the points on the vehicle. This produces 180 ($15 \times 4 \times 3$) images showing the visibility heatmap of points on the vehicle’s surface from a variety of angles. Since each *Grid Point* can only be recorded once per *Data Capture*, this color also represents the amount of circumstances under which a specific *Grid Point* was recorded.

In order to numerically process the data, each of the eight possible colors for a *Grid Point* was given an integer value, starting at 0 and ending at 7, this will be referred to as the *Visibility Index* of that point. Fig. 10, 11, and 12 show examples of the results for all four facings of the SUV vehicle at the three distance thresholds, with the appropriate coloring and *Visibility Index* labels.

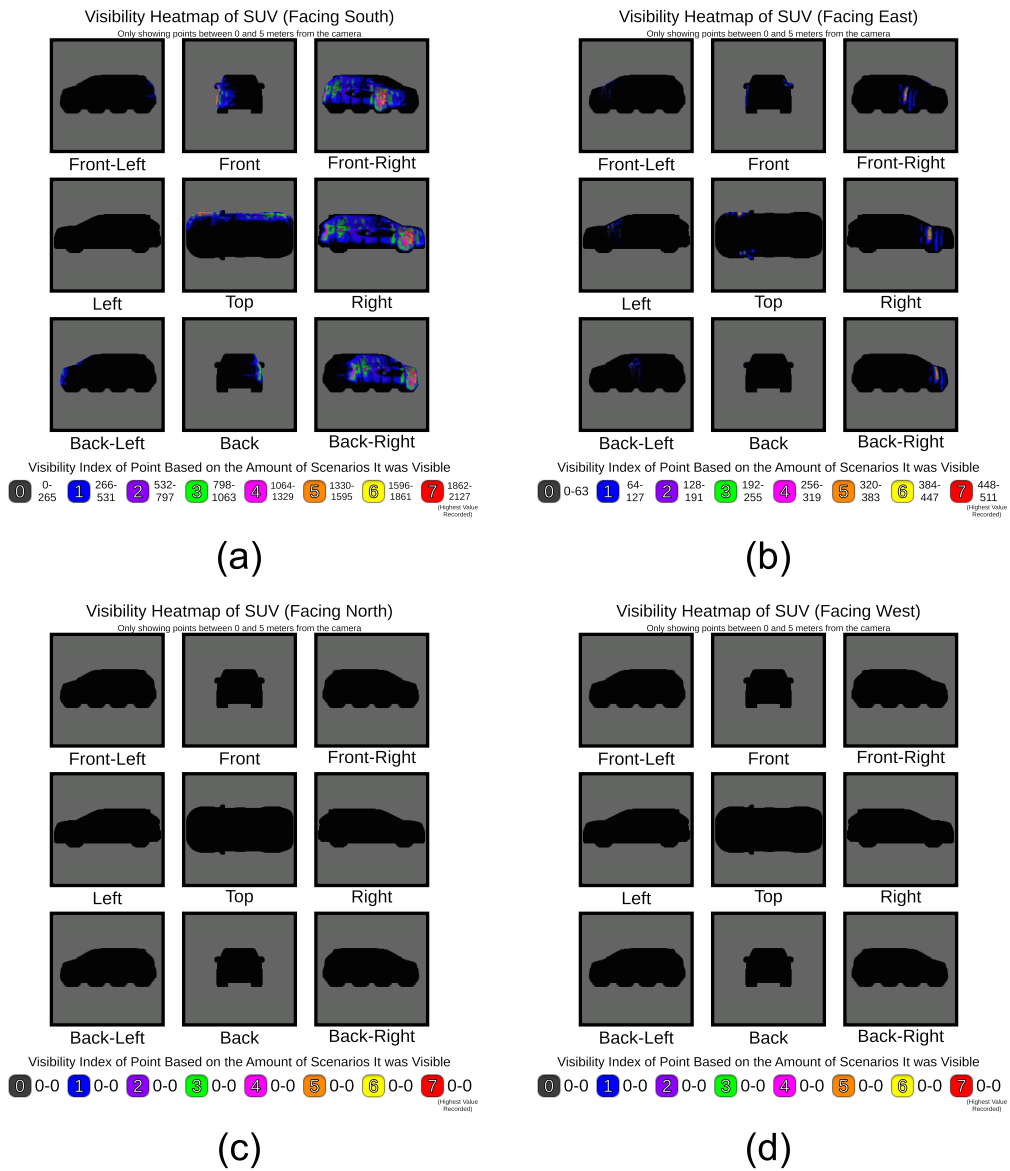


Fig. 10 Results showing how many times the *Grid Points* of the SUV vehicle was recorded, when these points are between 0m and 5m from the camera, and based on the direction the vehicle was driving: (a) Driving north, on the right side of the virtual environment; (b) driving east, out of the alleyway on the left side of the virtual environment; (c) driving south, on the left side of the virtual environment; (d) driving west, out of the alleyway on the right side of the virtual environment.

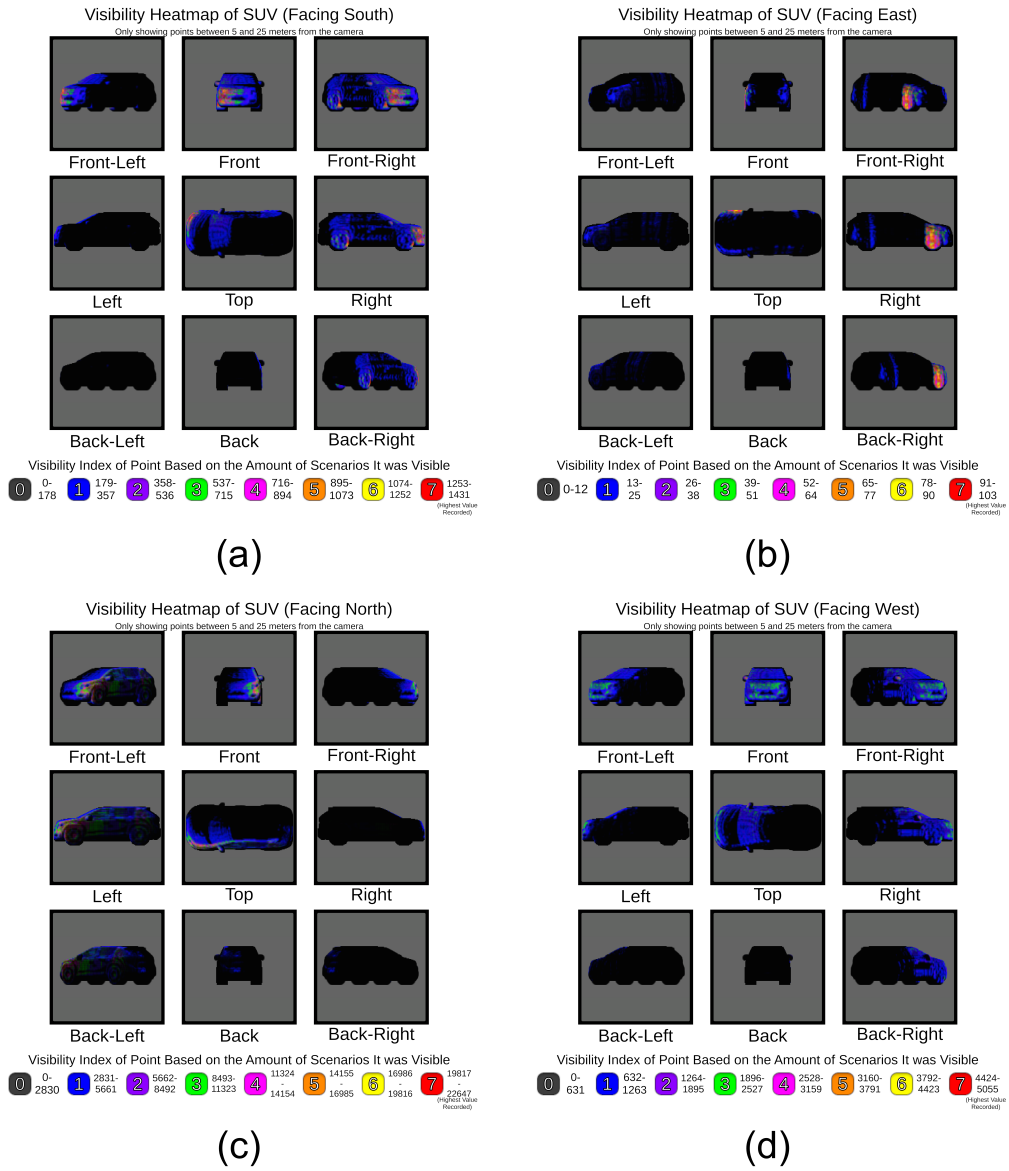


Fig. 11 Results showing how many times the *Grid Points* of the SUV vehicle was recorded, when these points are between 5m and 25m from the camera, and based on the direction the vehicle was driving: (a) Driving north, on the right side of the virtual environment; (b) driving east, out of the alleyway on the left side of the virtual environment; (c) driving south, on the left side of the virtual environment; (d) driving west, out of the alleyway on the right side of the virtual environment.

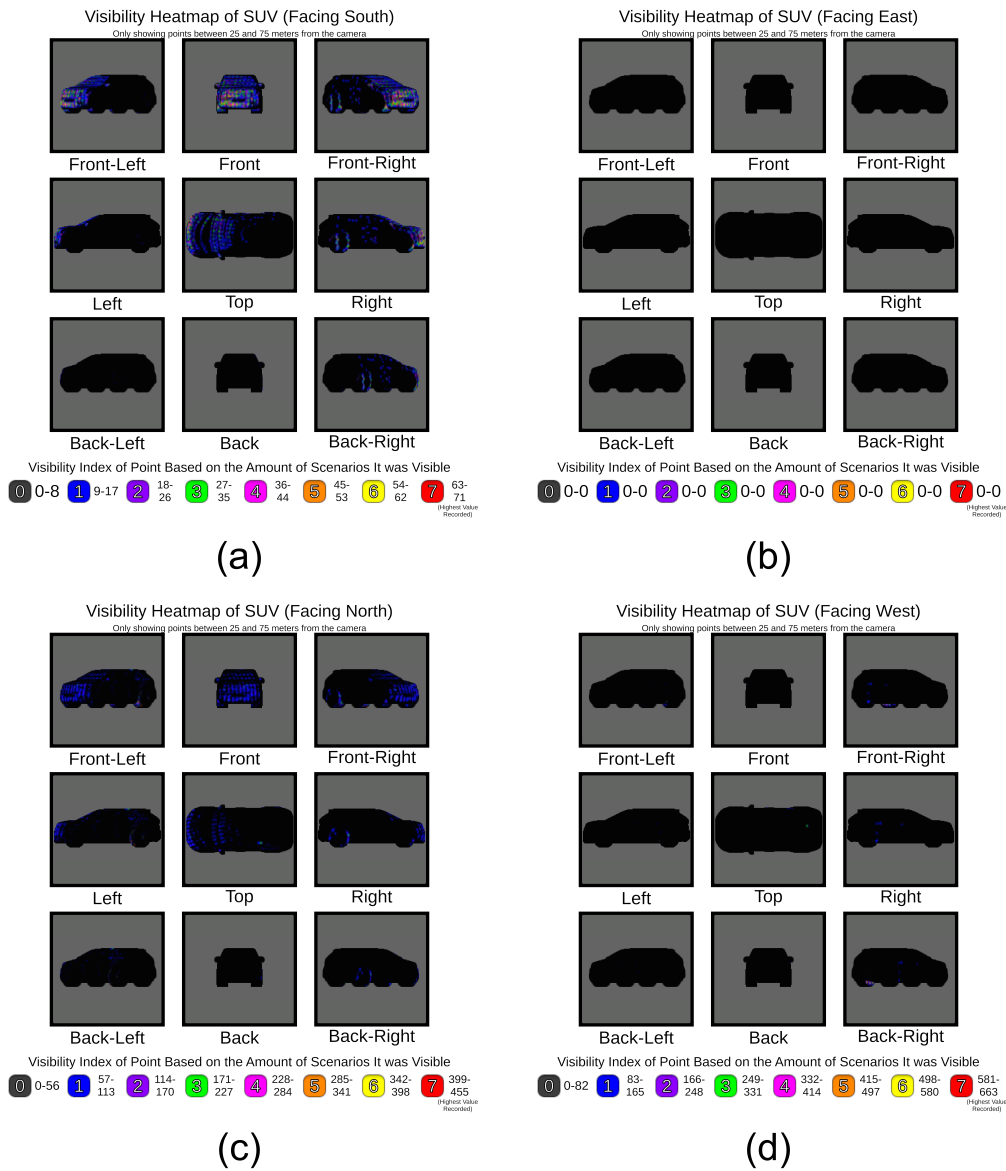


Fig. 12 Results showing how many times the *Grid Points* of the SUV vehicle was recorded, when these points are between 25m and 75m from the camera, and based on the direction the vehicle was driving: (a) Driving north, on the right side of the virtual environment; (b) driving east, out of the alleyway on the left side of the virtual environment; (c) driving south, on the left side of the virtual environment; (d) driving west, out of the alleyway on the right side of the virtual environment.

5.1 Data Analysis

During data analysis, we manually reviewed each of the 180 images to identify the visibility of each vehicle part. This required a visual aid and consistent terminology that could be used to identify each vehicle part, Fig. 13 provides both for the sedan vehicle type.

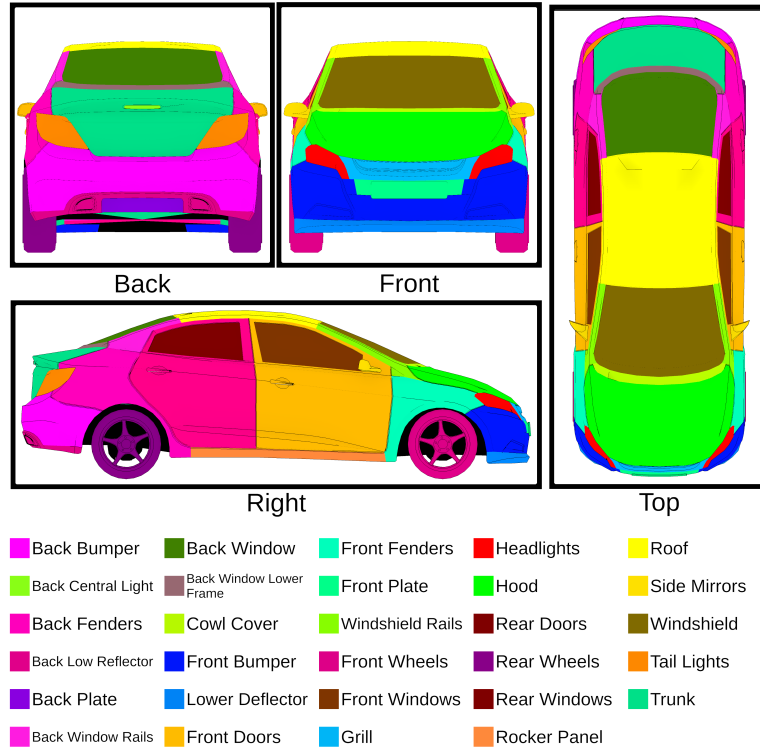


Fig. 13 Illustration of the different exterior parts of a sedan, and the terminology used to refer to each.

These parts were extrapolated for each of the 15 vehicle types, noting any time a part was not present in a vehicle type (e.g. doors on a motorcycle, roof on a convertible). Since the approach used for this study does not offer a way to measure the average color of a vehicle part, we only wrote down the highest *Visibility Index* found on each individual part, for each vehicle type and driving direction. This process was done three times, one for each distance range: 0m to 5m (Table 5), 5m to 25m (Table 6), and 25m to 75m (Table 7).

These tables show the highest recorded *Visibility Indices* for each part on each vehicle type. Each intersecting cell has four values separated by spaces, each value determining what the highest *Visibility Index* was for that part when that vehicle type was facing south, east, north, and west respectively. These cells are also shaded

based on the sum of their contents, with those closer to 28 (the maximum possible value) being darker. The column on the right shows the average of each row across all vehicles, and is shaded based on the smallest and largest value in that column. Whenever a vehicle does not feature the specified part, the intersecting cell is marked as "NA", which is valued the same as "0 0 0 0".

Highest registered visibility index on any point between 0 and 5 meters from the camera that is found on the part when the vehicle is in each of the four facings (South East North West).																
Vehicle Type & Part	Carryall Car	Double Decker Bus	Four Wheel Truck	Minibus	Motor-cycle	Motor Home	Moving Truck	Panel Van	Pickup Truck	Sedan	Single Decker Bus	Smart Car	Station Wagon	SUV	Topless Convertible	Avg. Highest
Back Bumper	3000	0100	0000	4000	0000	1000	0000	0000	1000	3000	0000	1100	5000	1000	4000	0.42
Back Central Light	NA	0000	NA	0000	NA	0000	NA	0000	0000	0000	0000	0000	0000	0000	NA	0
Back Fenders	4000	7000	NA	7000	3100	1000	3000	7000	4000	3000	1000	2200	7000	4000	3000	0.98
Back Low Reflector	NA	0000	1000	0000	NA	0000	NA	0000	1000	0000	0000	0000	0000	0000	0000	0.03
Back Plate	0000	0000	0000	0000	0000	0000	0000	0000	0000	0000	0000	0000	0000	0000	0000	0
Back Window Rails	1000	3000	NA	7000	NA	1000	NA	3000	1000	2000	0000	1100	3000	1000	NA	0.4
Back Window	NA	0000	NA	0000	NA	0000	NA	NA	3000	4000	0000	NA	0000	0000	NA	0.12
Back Window Lower Frame	NA	0000	NA	0000	NA	0000	NA	0000	0000	1000	0000	NA	0000	1000	NA	0.03
Cowl Cover	NA	2001	1000	1000	NA	0000	1000	0000	0000	1000	NA	1000	1200	0300	0300	0.28
Front Bumper	NA	5001	4500	4300	NA	6100	7000	2000	7000	5000	4000	1000	2000	2000	4000	1.05
Lower Deflector	NA	1001	3000	NA	NA	0000	0000	1000	4000	4000	NA	0000	NA	0000	0000	0.33
Front Doors	NA	NA	3600	4700	NA	1000	1100	4100	2100	4100	4700	7700	7100	4300	2200	1.33
Front Fenders	2200	5701	2100	2200	3300	4750	3500	7000	3700	5700	7100	3000	7700	6700	5300	2.15
Front Plate	0000	1000	0000	3000	NA	0000	5000	0000	0000	0000	0000	1000	0000	0000	0000	0.17
Front Wheels	2200	7101	4200	3700	3400	3100	4400	7300	3600	7500	1000	2100	7300	7700	7400	1.97
Front Windows	NA	3300	1100	7300	NA	2500	1100	3100	1100	3400	3700	7500	1100	1100	NA	1.1
Grill	NA	2000	3000	3100	NA	4000	7000	1000	5000	0000	3000	1000	1000	1000	1000	0.55
Headlights	0000	4201	3100	0300	3100	7000	4000	3000	4000	5000	3000	1000	7000	3000	0000	0.92
Hood	1100	NA	2000	1000	NA	3000	1100	1000	1000	1000	NA	1000	1100	1000	1000	0.3
Rear Doors	NA	NA	NA	7000	NA	NA	NA	4000	6000	4000	NA	NA	3000	3000	NA	0.5
Rear Wheels	1000	3000	5000	3000	3100	4000	1000	3000	1000	2000	1000	1100	3000	3000	2000	0.63
Rear Windows	NA	7000	NA	3000	NA	1000	NA	NA	3000	4000	4000	NA	3000	3000	NA	0.47
Rocker Panel	0000	NA	1000	0000	NA	1000	0000	0000	2000	0000	NA	1000	1000	0000	0000	0.15
Roof	4700	0001	2100	4100	NA	1000	2100	3000	1000	2100	0000	3300	3100	1000	NA	0.7
Side Mirrors	NA	0007	1000	7100	2300	3070	3100	4100	2100	4600	0070	1100	1000	4100	1000	1.15
Tail Lights	0000	0000	0000	2000	0000	7000	0000	6000	1000	1000	0000	0000	4000	1000	3000	0.42
Trunk	NA	NA	0000	1000	NA	0000	1000	0000	NA	1000	NA	0000	1000	1000	0000	0.08
Windshield	1000	3001	3100	1000	NA	1000	1300	1000	0100	1400	4000	1000	3100	1000	1100	0.57
Windshield Rails	2100	4001	1100	0200	NA	1000	1000	3600	3000	4300	7100	3400	4100	3500	3100	1.08

Table 5 The highest *Visibility Index* found on any point of each part, for each vehicle, for points between 0m and 5m away from the camera, and for each of the four driving directions of that vehicle (south, east, north, and west, respectively).

5.2 Effect of Distance

By separating the results based on the distance thresholds we can analyze how this distance may affect the visibility of certain elements. By comparing, for example, Fig. 11, 10, and 12, alongside Table 5, 6, and 7, we can make the following observations for the three ranges:

- 0m to 5m range:

Highest registered visibility index on any point between 5 and 25 meters from the camera that is found on the part when the vehicle is in each of the four facings (South East North West).																
Vehicle Type & Part	Carryall Car	Double Decker Bus	Four Wheel Truck	Minibus	Motor-cycle	Motor Home	Moving Truck	Panel Van	Pickup Truck	Sedan	Single Decker Bus	Smart Car	Station Wagon	SUV	Topless Convertible	Avg. Highest
Back Bumper	0000	0100	3010	6400	0000	0010	1010	0000	3010	0030	0000	0010	2040	0010	0030	0.6
Back Central Light	NA	0000	NA	0100	NA	0000	NA	0000	0000	0000	0010	0000	0010	0000	NA	0.05
Back Fenders	0141	2130	NA	3040	1133	1040	1010	1150	4230	1141	1110	5013	1150	2100	3130	1.43
Back Low Reflector	NA	0000	0010	0100	NA	0000	NA	0000	2000	0000	0000	0000	0000	0030	0000	0.12
Back Plate	0000	0000	0010	0000	0000	0010	0000	0000	0010	0010	0000	0000	0000	0010	0000	0.08
Back Window Rails	0344	1020	NA	1040	NA	0010	NA	0045	0020	0120	0000	0003	3142	1020	NA	0.83
Back Window	NA	0000	NA	0000	NA	0140	NA	NA	0110	0033	1100	NA	1051	0010	NA	0.38
Back Window Lower Frame	NA	0000	NA	0000	NA	0000	NA	0010	0010	0010	0000	NA	0010	0010	NA	0.08
Cowl Cover	NA	5077	2073	2013	NA	4073	1011	3113	2303	2523	NA	4233	0001	1003	2002	1.72
Front Bumper	NA	7377	3063	2473	NA	7074	3243	4374	4233	4557	7147	7067	4134	7243	7353	3.63
Lower Deflector	NA	4337	0030	NA	NA	1200	0000	1130	3133	3233	NA	4022	NA	2123	3001	1.37
Front Doors	NA	NA	1422	1353	NA	1000	1121	1133	2173	1444	2302	1762	2043	1043	2034	1.83
Front Fenders	1173	2773	1142	2331	5775	2072	1443	3773	4732	3774	6142	3353	2676	5763	7763	4.07
Front Plate	4023	2033	2033	1031	NA	4710	1033	1011	1001	3025	2023	4003	3013	3023	1001	1.58
Front Wheels	5575	3024	7243	4623	4556	3443	6753	4773	6733	3573	3010	3155	7754	5773	7772	4.35
Front Windows	NA	1704	1032	0000	NA	1173	1053	1033	2072	1747	1332	1652	1035	1033	NA	1.92
Grill	NA	4045	2033	1133	NA	4043	2033	3034	3013	4034	3014	4024	4027	4023	3011	2.02
Headlights	4063	6167	3064	2131	7137	7073	3074	3173	4133	4454	4037	4233	7057	7343	7344	3.73
Hood	1124	NA	2033	1011	NA	4043	1132	3112	1121	2334	NA	4013	1212	2221	1222	1.48
Rear Doors	NA	NA	1160	NA	NA	NA	NA	1120	1140	1037	NA	NA	2031	1031	NA	0.67
Rear Wheels	1042	4530	7771	7730	2113	3040	7071	7141	4450	4031	3210	5025	5032	7131	7131	2.88
Rear Windows	NA	1430	NA	1000	NA	1010	NA	NA	3131	1034	2330	NA	1051	2231	NA	0.83
Rocker Panel	4470	NA	2040	0001	NA	0050	1010	0000	1041	0003	NA	0331	0000	0040	0000	0.82
Roof	2752	2213	2331	0213	NA	1044	1043	1032	1042	1234	4354	1332	2144	1021	NA	1.98
Side Mirrors	NA	7075	4253	4017	7633	7077	4037	5057	7057	4055	7162	3223	5036	5147	7037	3.72
Tail Lights	0000	0000	0000	0000	0000	0010	0000	0000	4010	0040	0000	0003	0000	0000	0000	0.22
Trunk	NA	NA	0000	0200	NA	0030	0010	0000	NA	0030	NA	0010	0010	0010	0020	0.23
Windshield	7047	7177	2032	2023	NA	4374	1013	2114	2013	2125	4074	4222	3024	3013	2032	2.48
Windshield Rails	3337	5174	1171	1313	NA	1332	1033	3343	2063	3255	3273	1252	3044	1143	2153	2.7

Table 6 The highest *Visibility Index* found on any point of each part, for each vehicle, for points between 5m and 25m away from the camera, and for each of the four driving directions of that vehicle (south, east, north, and west, respectively).

- The five parts with the highest average registered *Visibility Index* are the front fenders (2.15), front wheels (1.97), side mirrors (1.14), front windows (1.10), and windshield rails (1.08).
- Whenever the vehicle is on the right lane or right alleyway they are also usually further than 5m away from the camera, so they are rarely captured. The only exceptions to this were the double decker bus when facing west, and the motor home and single decker bus when facing north.
- **5m to 25m range:**
 - The five parts with the highest average registered *Visibility Index* are the front wheels (4.35), front fenders (4.07), headlights (3.73), side mirrors (3.72), and rear wheels (2.88).
 - At this distance we see higher *Visibility Indices* on average and a wider distribution of higher values across parts.
- **25m to 75m range:**

Highest registered visibility index on any point between 25 and 75 meters from the camera that is found on the part when the vehicle is in each of the four facings (South East North West).																
Vehicle Type & Part	Carryall Car	Double Decker Bus	Four Wheel Truck	Minibus	Motor-cycle	Motor Home	Moving Truck	Panel Van	Pickup Truck	Sedan	Single Decker Bus	Smart Car	Station Wagon	SUV	Topless Convertible	Avg. Highest
Back Bumper	0000	0000	0007	7035	0000	2004	1010	0002	0007	3030	1500	2000	0003	0000	0003	0.38
Back Central Light	NA	0000	NA	1000	NA	0000	NA	0000	1000	0000	0000	0000	0031	0000	NA	0.08
Back Fenders	0007	2034	NA	4013	0030	4003	1003	0052	2077	6061	1714	0051	2031	0010	0032	1
Back Low Reflector	NA	0000	0003	0000	NA	0000	NA	0000	0000	2000	0000	0000	0000	0000	0000	0.03
Back Plate	0000	0000	0000	1001	0000	3000	0000	0000	0000	1000	0000	0000	4034	0000	2011	0.25
Back Window Rails	3020	0004	NA	2016	NA	0000	NA	0004	1011	1020	7734	0004	7071	0000	NA	0.62
Back Window	NA	2005	NA	1001	NA	1000	NA	NA	1011	3033	0400	NA	1013	0000	NA	0.23
Back Window Lower Frame	NA	0000	NA	1001	NA	0000	NA	0000	0000	1010	0000	NA	0010	0000	NA	0.07
Cowl Cover	NA	3040	0000	2000	NA	4070	0000	2000	1000	3000	NA	0030	3010	3010	2010	0.67
Front Bumper	NA	3050	3000	4020	NA	4060	1000	7000	3000	7010	3030	0000	7010	7030	7020	1.32
Lower Deflector	NA	2030	0000	NA	NA	0000	1000	2000	1000	4010	NA	0000	NA	3000	3010	0.35
Front Doors	NA	NA	3020	3014	NA	0010	0000	4000	4011	1010	3023	3000	1010	3021	4010	0.68
Front Fenders	0000	3040	0000	6010	0040	0010	0000	4000	3030	4010	2000	0020	3010	6010	7010	0.95
Front Plate	0000	3050	0000	4020	NA	7030	2000	0000	0000	4010	3010	0000	4000	6030	3010	0.87
Front Wheels	0020	4034	3030	4024	0050	5071	3000	4000	4000	3010	3031	0070	7010	6020	5020	1.48
Front Windows	NA	3000	3010	1034	NA	5032	0025	2000	3021	3010	0001	2000	1010	2010	NA	0.65
Grill	NA	3050	2000	4020	NA	5040	3000	5000	3000	7010	2020	0000	7020	7020	0010	1.12
Headlights	0000	3040	3000	7010	0070	4070	3000	4000	3000	4010	2030	0050	7020	7030	4020	1.43
Hood	0000	NA	1000	3010	NA	4070	1000	4000	1000	4010	NA	0000	3000	3010	3010	0.63
Rear Doors	NA	NA	NA	3001	NA	NA	NA	3040	3000	4000	NA	NA	2031	2011	NA	0.42
Rear Wheels	2020	7037	7064	7077	3020	4022	7047	7057	5057	3064	3033	7026	3047	6077	6065	2.35
Rear Windows	NA	2004	NA	5034	NA	3013	NA	NA	1010	2017	2777	NA	1043	0010	NA	0.57
Rocker Panel	0000	NA	7000	0000	NA	0001	0004	0040	3012	2000	NA	1000	0001	0000	0000	0.3
Roof	2030	3033	0000	2023	NA	7041	3010	1012	1011	2002	1723	2040	2063	3033	NA	0.98
Side Mirrors	NA	3041	3000	3023	0000	5071	3000	6000	6033	1000	1040	0070	2000	6020	4020	1.23
Tail Lights	0000	0000	0000	2000	0000	0000	0000	0000	0000	3030	0000	0000	0000	0000	0002	0.13
Trunk	NA	NA	0000	3005	NA	0000	3000	0000	NA	1013	NA	1000	1011	0000	3011	0.25
Windshield	0070	3070	1000	4020	NA	4070	3020	4000	3010	3010	3030	0030	3020	6010	3010	1.28
Windshield Rails	0050	0000	0000	4020	NA	1001	1000	2000	3020	3010	3010	0030	3010	4010	3010	0.73

Table 7 The highest *Visibility Index* found on any point of each part, for each vehicle, for points between 25m and 75m away from the camera, and for each of the four driving directions of that vehicle (south, east, north, and west, respectively).

- The five parts with the highest average registered *Visibility Index* are the rear wheels (2.35), front wheels (1.48), headlights (1.43), front bumper (1.32), and windshield (1.28).
- At this distance we see a drop in resolution, product of the Inverse Square Law. This is particularly noticeable with the motorcycle and the carryall car, which are missed by the ray-casts due to their size.

Noticeably, only the front fenders and front wheels are present across all distances. However, one must remember the findings of [6], and how pedestrians lost their willingness to cross the road when the vehicle was 40m away from them. This points to the 25m to 75m range as particularly important results to consider, specially since it also includes the windshield and front bumper, which both [6] and [5] determined to be high areas of interest for pedestrians.

Average highest visibility index on vehicle part when it is facing...					
Direction	North	East	South	West	Average
Back Bumper	0.51	0.27	1.2	0.69	0.67
Back Central Light	0.17	0.03	0.07	0.03	0.08
Back Fenders	1.88	0.5	2.48	1.1	1.49
Back Low Reflector	0.11	0.03	0.17	0.08	0.1
Back Plate	0.2	0	0.24	0.13	0.14
Back Window Rails	1.24	0.39	1.52	1.15	1.08
Back Window	0.79	0.29	0.75	0.71	0.64
Back Window Lower Frame	0.26	0	0.15	0.04	0.11
Cowl Cover	1.28	0.53	1.64	1	1.11
Front Bumper	2.33	0.9	4.49	1.51	2.31
Lower Deflector	0.87	0.42	1.78	0.84	0.98
Front Doors	1.44	1.69	2.44	1.08	1.67
Front Fenders	2.4	2.82	3.31	1.02	2.39
Front Plate	0.93	0.17	1.86	0.79	0.93
Front Wheels	2.42	2.67	4.18	1.36	2.66
Front Windows	1.58	1.58	1.94	1.36	1.62
Grill	1.31	0.05	3.1	1.21	1.42
Headlights	2.38	0.53	3.78	1.42	2.03
Hood	1	0.44	1.81	0.78	1.01
Rear Doors	1.61	0.17	2.84	0.67	1.32
Rear Wheels	2.6	0.69	4.13	2.02	2.36
Rear Windows	1.63	0.71	2.33	1.46	1.53
Rocker Panel	0.92	0.19	0.81	0.39	0.58
Roof	1.85	1.15	1.9	1.46	1.59
Side Mirrors	2.48	0.64	3.62	2.17	2.23
Tail Lights	0.2	0	0.76	0.11	0.27
Trunk	0.5	0.07	0.57	0.33	0.37
Windshield	1.9	0.45	2.55	1.29	1.55
Windshield Rails	1.93	1.12	2.29	1.14	1.62

Table 8 The average highest Visibility Index found on each part, for each facing direction. On the right we see the total average of the part across all four directions.

5.3 Parts Visible Most Often

Based on the data observed across Table 5, 6, and 7, the following vehicle parts stand out as having the highest

5.4 Effects of Vehicle Position

Table 8 summarizes the average highest *Visibility Index* for each part, alongside the average of these averages.

Based on this data, we can determine that the position of the vehicle plays an important role in determining visibility, and make the following observations:

- Elements placed on the back of the vehicle such as the back central light, back bumper, back plate, back window, back window lower frame, tail lights, and trunk perform poorly in all four scenarios. This is to be expected, as the setup of the

experiment focused on *Camera Directions* where the pedestrian could see the front of the vehicle.

- Most elements perform worse when the vehicle is in the alleyway intersecting the sidewalk, with the exception of the front doors, front fenders, front wheels, and front windows.
- The five parts with the highest recorded *Visibility Index* for each facing direction are:
 - **North:** Rear wheels (2.6), side mirrors (2.48), front wheels (2.42), front fenders (2.4), and headlights (2.38).
 - **East:** Front fenders (2.82), front wheels (2.67), front doors (1.69), front windows (1.58), and roof (1.15).
 - **South:** Front bumper (4.49), back fenders (4.48), front wheels (4.18), rear wheels (4.13), and headlights (3.78).
 - **West:** Side mirrors (2.17), rear wheels (2.02), front bumper (1.51), rear windows (1.46), and roof (1.46).

5.5 Parts Visible Most Often

Using Table 8, we can determine that the five parts with the highest average across the four directions are the front wheels (2.66), front fenders (2.39), rear wheels (2.36), front bumper (2.31), and side mirrors (2.23).

5.6 Limitations of Study

Since this is a study that makes use of ray-casting to determine the visibility of objects, it does not account for non-geometrical factors that may affect how well a pedestrian may perceive an element of a vehicle. This includes reflections, such as the one from glass or chrome details, as well as the color and finish of the vehicle. This study also does not account for other visual difficulties such as poor weather, low light conditions, or visual imparity.

Additionally, since the program makes use of models freely available on Sketchfab, the level of detail between them is not consistent, and some are of much lower poly-count than others. This is relevant, as the simulation relies entirely on the geometry of the objects, and a lower level of detail may signify much less clear results for some of the vehicle types.

Finally, this study was done entirely with static vehicles. While the number of *Camera Positions* and *Camera Directions* was chosen to simulate the different possible angles that a pedestrian may encounter a vehicle, it does not fully replicate the changes in vehicle rotation or motion that may alter the perspective of the viewer.

5.7 Discussion

Despite the study from Troel-Madec et al. [7] pointing to the front doors and windshield rails as ideal placements for external human-machine interfaces (eHMI), the former is only highlighted to have a high *Visibility Index* when the vehicle is coming out of an alleyway, and the latter when the vehicle is between 0m and 5m away from

the camera. This difference in results is likely due to the larger variety of vehicle types and permutations of occlusion scenarios present in our study.

On the other hand, their conclusion that the side of the vehicle is a good placement for eHMIs is backed by the present research, as the wheels, fenders, and side mirrors show to be relevant in multiple occasions. This also aligns with the findings that moving elements of the vehicle such as vehicle wheels to be points of interest for pedestrians [8].

Two other parts with high *Visibility Indices* are the front bumper and headlights, one of which already features a signaling device in the form of turning lights. This is consistent with findings that pedestrians focus on the front of the vehicle during crossing events [5, 6, 8].

Noticeably, the *Visibility Index* of the windshield only stands out once when the vehicle is in the 25m to 75m range, which does bring attention to the observation that pedestrians lose the confidence to cross a road as a vehicle approaches within 40m[6] of them. This noteworthy, as previous studies have consistently found that the gaze of pedestrians naturally gravitate towards the windshield of vehicles, while this study reveals that it is also area easily occluded by other elements on the road.

Another factor to consider is how the effects of the Inverse Square Law, as observed in Fig. 7, informs us of a need for large displays on autonomous vehicles in order to communicate at long distances. This means that we must prioritize placement of eHMIs that allow us to implement larger displays. This is particularly important for smaller vehicles.

Our results suggest that a distributed approach to eHMI placement is required to fulfill both the behavioral response of pedestrians and ensure that signaling is as visible as often as possible. Based on the results presented in Table 8, previous research, and the items previously discussed, the recommended placement for eHMIs would be at least one of the following pairs:

- **Windshield and front fender:** Provides two large surfaces to place displays. Works for vehicle types such as a sedan, SUV, panel van, topless convertible, station wagon, minibus, pickup truck, motor home, or bus.
- **Windshield and side mirrors:** Provides one large surface to place a display and a secondary smaller one. Works for vehicle types such as a smart car, carryall car, sedan, SUV, panel van, topless convertible, station wagon, four wheel truck, minibus, pickup truck, moving truck, motor home, or a bus.
- **Front bumper and fender:** Provides two large surfaces to place displays. Works best for vehicle types such as a sedan, SUV, panel van, topless convertible, station wagon, minibus, pickup truck, motor home, or bus.
- **Front bumper and front wheel:** Provides one large surface to place a display and a smaller, but still significant one. Works for vehicle types such as a motorcycle, smart car, sedan, SUV, panel van, topless convertible, station wagon, four wheel truck, minibus, pickup truck, motor home, or bus. May be expensive to install.
- **Front fender and side mirrors:** Provides one large surface to place a display and a secondary smaller one. Works for vehicle types such as a motorcycle, sedan, SUV, panel van, topless convertible, station wagon, minibus, pickup truck, motor home, or bus. Does not provide a position usually gazed by pedestrians.

While these suggestions contradict the conclusion that eHMI placement should be standardized [8], it bridges the gaps between the results of behavioral studies on pedestrian response and concerns of visibility.

6 Future Work

This paper aims to generate knowledge on the general visibility of different parts of the vehicles tested. The results represent those obtained under very specific circumstances, and more specific patterns may arise if changes are made to it.

Some future iterations of this experiment may find data for left-hand driving, find the visibility heat map of vehicles in respect to other drivers, include autonomous vehicle models, include and evaluate parts associated to autonomous vehicles (e.g. sensor pods), focus on the back of the vehicles, or add different obstacles such as traffic signs and parked vehicles. Different layouts could also be tested, making changes to the currently used one such as widening the sidewalk, adding biking lane between the vehicles and the sidewalk, increasing the amount of lanes, adding a traffic light intersection, et cetera.

This study is entirely limited to measuring the visibility of the geometry of objects, and does not test other factors that might compromise visibility such as color and reflections. The software used is also entirely static, and does not feature an animation system that might affect the results. Additional work may include testing different visibility conditions, testing the recommended external human-machine interface placements in a virtual reality experiment, or introducing an animation of a vehicle in motion to collect data on how its visibility changes.

Future work can also be done to design an experiment capable of measuring the value of points on a given part and produce a total for each, instead of requiring manual analysis and using only the maximum values found.

7 Conclusion

In this paper, we used a virtual simulation to determine the most visible parts of fifteen different incoming vehicles of drastically different shapes and sizes, when placed at multiple points in a two-way two-lane right-driving street with sidewalks. The results point to the frontal fenders and the headlights as the best placement for eHMIs communicating the intent of an incoming vehicle, with the front wheels, front doors, front bumper, and side mirrors as less visible alternatives.

While not particularly concurrent with the results and observations by [7], it correlates with already-existing forms of signaling in modern vehicles. Additional testing might prove useful to better understand and contextualize these findings, but the data revealed in this experiment is valuable to design better forms of signaling in our modern roads that can be seen by their intended audience, especially as we steadily keep progressing to a future where autonomous vehicles roam our cities.

8 Declarations

8.1 Funding

Jaerock Kwon is an associate professor for University of Michigan Dearborn. Jose Gonzalez-Belmonte is an assistant professor for Lawrence Technological University, and his ongoing studies are being partially funded by it. The authors did not receive support from any other organization for the submitted work.

8.2 Conflict of Interest

The author of this paper declares that they have no known competing financial interests or personal relationships that could have appeared to influence the work reported in this paper.

8.3 Ethics approval and consent to participate

Not applicable.

8.4 Consent for publication

Not applicable.

8.5 Data availability

The data produced and used for this paper can be found at <https://jgonzalez-uom.github.io/visibility/>

8.6 Materials availability

The software used for this paper, along with a manual to use it, can be found at <https://jgonzalez-uom.github.io/visibility/>

8.7 Code availability

The source code of the software used for this paper can be found at <https://github.com/jgonzalez-uom/ReadabilityModel/> The latest commit for the repository as of the time of writing was made on January 17 at 3:23AM. The code is fully functional.

8.8 Author contribution

All authors contributed to the study conception and design. Material preparation, software development, data collection, and analysis were performed by Jose Gonzalez-Belmonte. The first draft of the manuscript was written by Jose Gonzalez-Belmonte, and Jaerock Kwon commented and suggested edits on previous versions of the manuscript. All authors have read and approved the final manuscript.

8.9 Acknowledgements

Not applicable.

References

- [1] Winter, J., Dodou, D.: External human–machine interfaces: Gimmick or necessity? *Transportation Research Interdisciplinary Perspectives* **15**, 100643 (2022) <https://doi.org/10.1016/j.trip.2022.100643> . Accessed 2024-03-16
- [2] Clercq, K., Dietrich, A., Núñez Velasco, J.P., Winter, J., Happee, R.: External Human-Machine Interfaces on Automated Vehicles: Effects on Pedestrian Crossing Decisions. *Human Factors* **61**(8), 1353–1370 (2019) <https://doi.org/10.1177/0018720819836343> . Accessed 2024-03-16
- [3] Rodríguez Palmeiro, A., Kint, S., Vissers, L., Farah, H., Winter, J.C.F., Hagenzieker, M.: Interaction between pedestrians and automated vehicles: A Wizard of Oz experiment. *Transportation Research Part F: Traffic Psychology and Behaviour* **58**, 1005–1020 (2018) <https://doi.org/10.1016/j.trf.2018.07.020> . Accessed 2024-03-16
- [4] Alhawiti, A., Kwigizile, V., Oh, J.-S., Asher, Z.D., Hakimi, O., Aljohani, S., Ayantayo, S.: The Effectiveness of eHMI Displays on Pedestrian–Autonomous Vehicle Interaction in Mixed-Traffic Environments. *Sensors (Basel, Switzerland)* **24**(15), 5018 (2024) <https://doi.org/10.3390/s24155018> . Accessed 2024-10-08
- [5] Guo, F., Lyu, W., Ren, Z., Li, M., Liu, Z.: A Video-Based, Eye-Tracking Study to Investigate the Effect of eHMI Modalities and Locations on Pedestrian–Automated Vehicle Interaction. *Sustainability* **14**(9), 5633 (2022) <https://doi.org/10.3390/su14095633> . Number: 9 Publisher: Multidisciplinary Digital Publishing Institute. Accessed 2024-03-16
- [6] Dey, D., Walker, F., Martens, M., Terken, J.: Gaze Patterns in Pedestrian Interaction with Vehicles: Towards Effective Design of External Human-Machine Interfaces for Automated Vehicles. In: *Proceedings of the 11th International Conference on Automotive User Interfaces and Interactive Vehicular Applications. AutomotiveUI '19*, pp. 369–378. Association for Computing Machinery, New York, NY, USA (2019). <https://doi.org/10.1145/3342197.3344523> . <https://dl.acm.org/doi/10.1145/3342197.3344523> Accessed 2026-01-16
- [7] Troel-Madec, M., Boissieux, L., Borkowski, S., Vaufreydaz, D., Alaimo, J., Chatagnon, S., Spalanzani, A.: eHMI positioning for autonomous vehicle/-pedestrians interaction. In: *Adjunct Proceedings of the 31st Conference on L'Interaction Homme-Machine. IHM '19 Adjunct*, pp. 1–8. Association for Computing Machinery, Grenoble, France (2019). <https://doi.org/10.1145/3366551.3370340> . <https://hal.science/hal-02388847> Accessed 2024-03-16

- [8] Winter, J., Bazilinsky, P., Wesdorp, D., Vlam, V., Hopmans, B., Visscher, J., Dodou, D.: How do pedestrians distribute their visual attention when walking through a parking garage? An eye-tracking study. *Ergonomics* **64**(6), 793–805 (2020)
- [9] Aversa, D.: *Unity Artificial Intelligence Programming : Add Powerful, Believable, and Fun AI Entities in Your Game with the Power of Unity*, Fifth edition edn. Packt Publishing, Birminham, UK (2022)
- [10] Federal Highway Administration: Office of Highway Policy Information - Policy | Federal Highway Administration. https://www.fhwa.dot.gov/policyinformation/tmguides/tmg_2013/vehicle-types.cfm Accessed 2024-05-24
- [11] [@Alex.Ka.]: Honda Shadow RS 2010 (2022). <https://sketchfab.com/models/2e7cf7bc195044f4a0f60c04581e2691/embed?autostart=1> Accessed 2024-10-16
- [12] [@beztao01]: Smart By Material (2021). <https://sketchfab.com/models/27a7f393d3134e90b30d03bc6805cfb1/> Accessed 2024-10-16
- [13] [@maxdragon]: area 9 golf cart (2021). <https://sketchfab.com/models/5fd13a5303af4f3bbba993dad35f788/> Accessed 2024-10-16
- [14] Daniel Zhabotinsky [@DanielZhabotinsky]: Generic sedan 2010 (2020). <https://sketchfab.com/models/7fd6e15785fa4aa9bfd6e31eb7c97ba6/> Accessed 2024-10-16
- [15] [@fishermans]: Ford Edge 2006 lowpoly for 3D-printing (2024). <https://sketchfab.com/models/dec7fe5f75874a9cb913e8e54dcd4954/> Accessed 2024-10-16
- [16] [@danzzzeg]: D3S MB Vito Panel Van (W447) '15 (2017). <https://sketchfab.com/models/98d85b403ba0426f84636b575319e4f7/> Accessed 2024-10-16
- [17] [Brian N.]: Chrysler Sebring Convertible (2007). <https://sketchfab.com/3d-models/chrysler-sebring-convertible-dac8529f24754bbd936173cbe8da92b1> Accessed 2024-10-16
- [18] Daniel Zhabotinsky [@DanielZhabotinsky]: American 80s Station Wagon - Low poly model (2020). <https://sketchfab.com/models/680e4ad1090f4e738bbd46e618f3a01f/> Accessed 2024-10-16
- [19] Daniel Zhabotinsky [@DanielZhabotinsky]: Light Box Truck - Low poly model (2020). <https://sketchfab.com/models/cbc508a5ad424d79b2f2c8a3de7e1cd3/> Accessed 2024-10-16
- [20] [@boitaloran]: Peugeot J5 Minibus (2022). <https://sketchfab.com/models/55d72c5dd507464ca2fe26f782f8c04e/> Accessed 2024-10-16
- [21] David Holiday [@David.Holiday]: 2015 Ford F150 King Ranch Edition (2021).

- <https://sketchfab.com/models/79ebd5caaf414ab08debc36157dbc878/> Accessed 2024-10-16
- [22] Daniel Zhabotinsky [@DanielZhabotinsky]: '90 Light Commercial Truck - Low poly model (2021). <https://sketchfab.com/models/663a0953c038434a918cb85725c88ffa/> Accessed 2024-10-16
- [23] Lion Sharp [@lionsharp]: FREE GMC Motorhome reimaged low poly (2013). <https://sketchfab.com/models/6hiH0iyDqXqtdD9wbqSbyLLhKmz/> Accessed 2024-10-16
- [24] [@businessyuen]: Bus (2020). <https://sketchfab.com/models/cc159e95590b49999c6e08793eb0a76a/> Accessed 2024-10-16
- [25] [@own.guest]: Generic Town Bus (2021). <https://sketchfab.com/models/14fe03d792914d51b6c6250b393c44fd/> Accessed 2024-10-16
- [26] National Center for Health Statistics: Growth Charts - Clinical Growth Charts (2024). <https://www.cdc.gov/growthcharts/data/set1clinical/cj41c021.pdf> Accessed 2026-01-16
- [27] W3Counter: Global Web Stats - August 2024 (2024). <https://www.w3counter.com/globalstats.php?year=2024&month=8> Accessed 2026-01-16
- [28] Browson, J.R.S.: Laws of Light (2014). <https://doi.org/10.1016/B978-0-12-397021-3.00003-X> . <https://www.sciencedirect.com/science/chapter/monograph/pii/B978012397021300003X> Accessed 2026-01-16